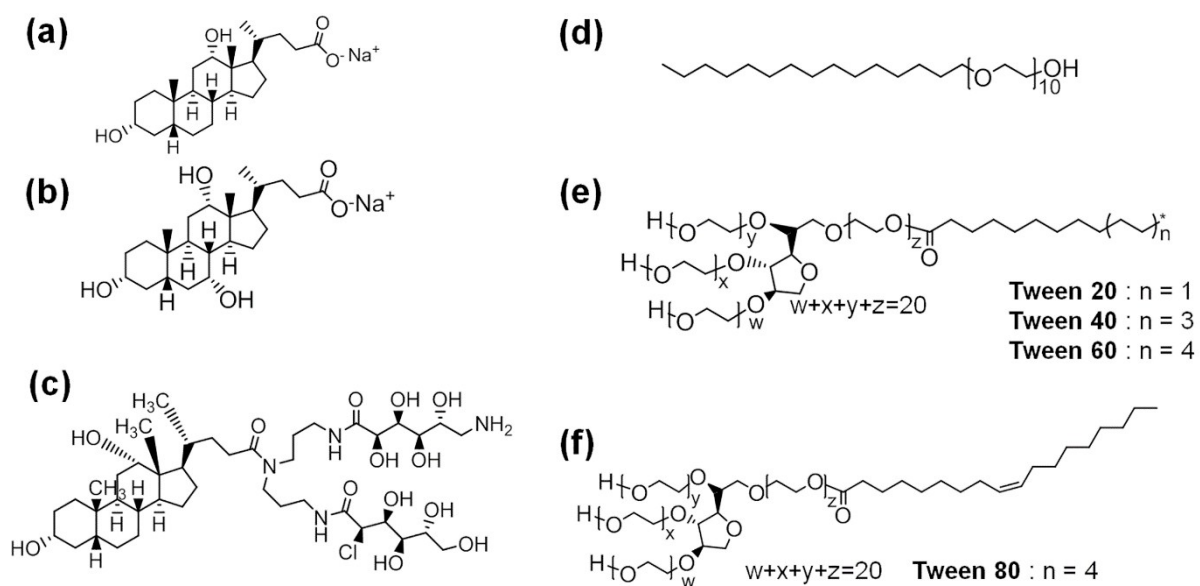


## Electronic Supplementary Information

### Universal selection rule for surfactants used in miniemulsion processes for eco-friendly polymer semiconductors

Jangwhan Cho, Seongwon Yoon, Kyu Min Sim, Yong Jin Jeong, Chan Eon Park, Soon-Ki Kwon, Yun-Hi Kim\* and Dae Sung Chung\*



**Figure S1.** Chemical structures of (a) Sodium cholate (SC), (b) sodium dedoxycholate, (c)  $N,N$ -Bis[3-(D-gluconamido)propyl]deoxycholamide, (d)  $C_{16}E_{10}$  (e) Tween 20 ( $n=1$ ), Tween 40 ( $n=3$ ), Tween 60 ( $n=4$ ), (f) Tween 80.

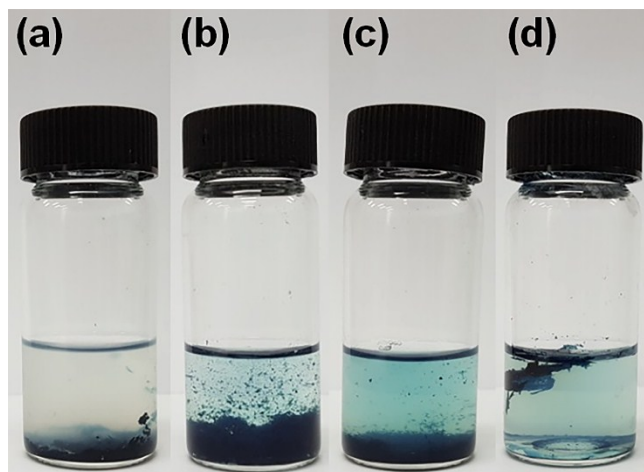


**Figure S2.** The digital camera images of (a)  $C_{12}E_4$ -, (b)  $C_{16}E_{10}$ -, (c) Triton X-100- and (d) SC-based colloid solutions fabricated by miniemulsion method. All these colloid solutions were unstable with large clusters.

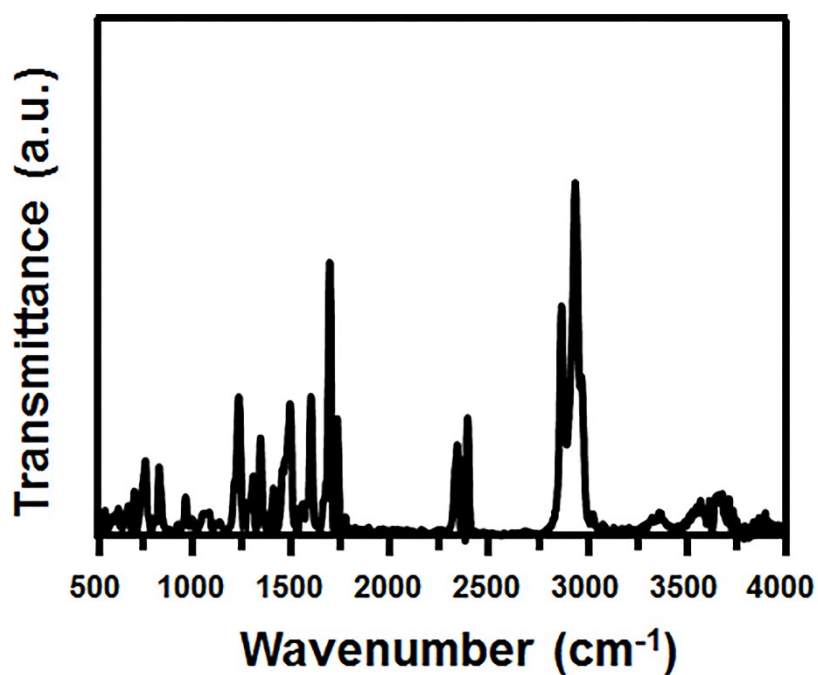


**Figure S3.** FT-IR spectrum of PNDI-TVT film fabricated from dichlorobenzene solution.

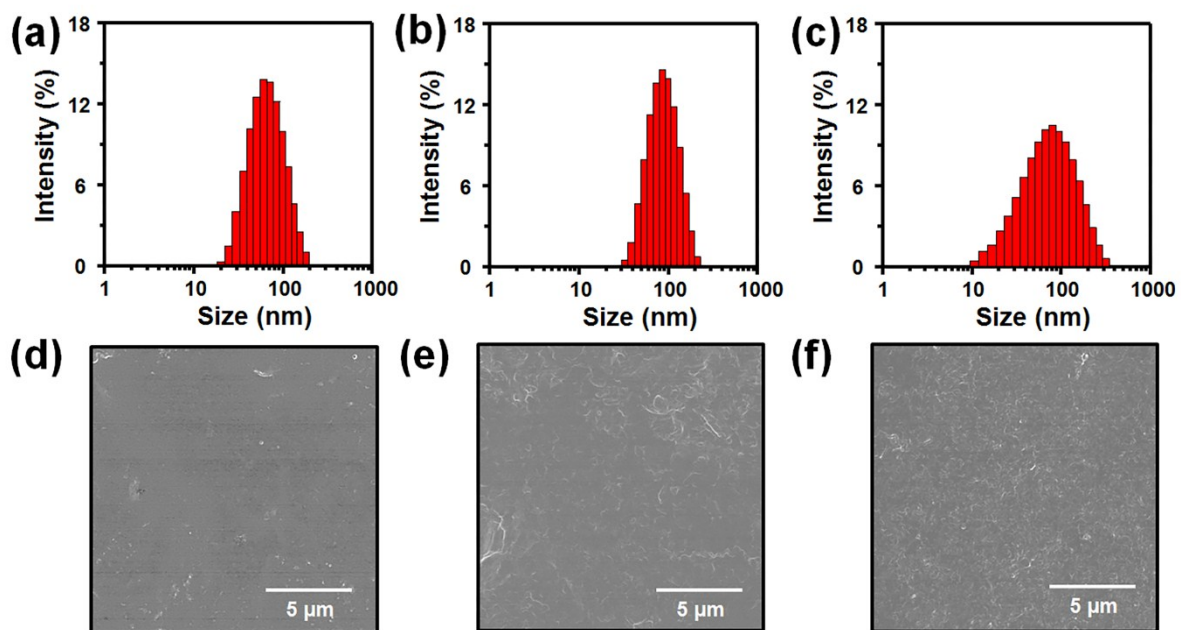


**Figure S4.** (a-c) Size distributions for C<sub>10</sub>TAB-, C<sub>14</sub>TAB- and C<sub>16</sub>TAB-based colloid of PNDI-TVTV in a dilute solution measured by dynamic light scattering (DLS) method. (d-f) the SEM images of C<sub>10</sub>TAB-, C<sub>14</sub>TAB- and C<sub>16</sub>TAB-based colloid films deposited by spray coating.

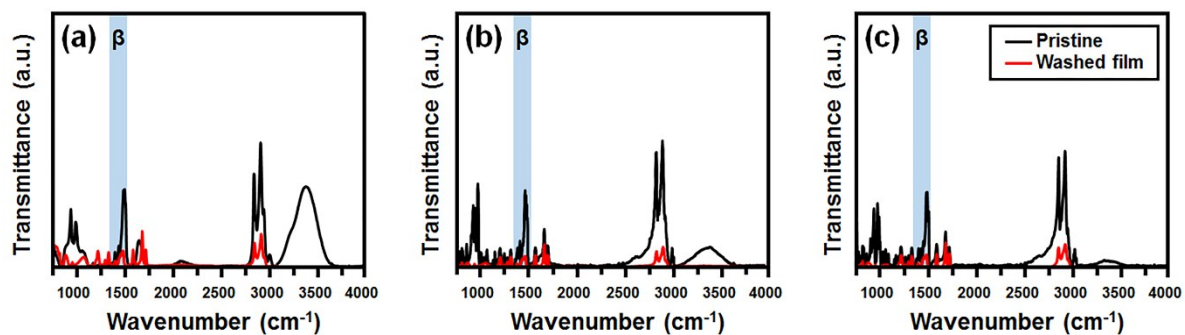


**Figure S5.** FT-IR spectra of C<sub>10</sub>TAB-, C<sub>14</sub>TAB- and C<sub>16</sub>TAB-based colloid films before and after post-treatment for washing: β (1320-1500 cm<sup>-1</sup>) region corresponds to stretching vibration of C–N.

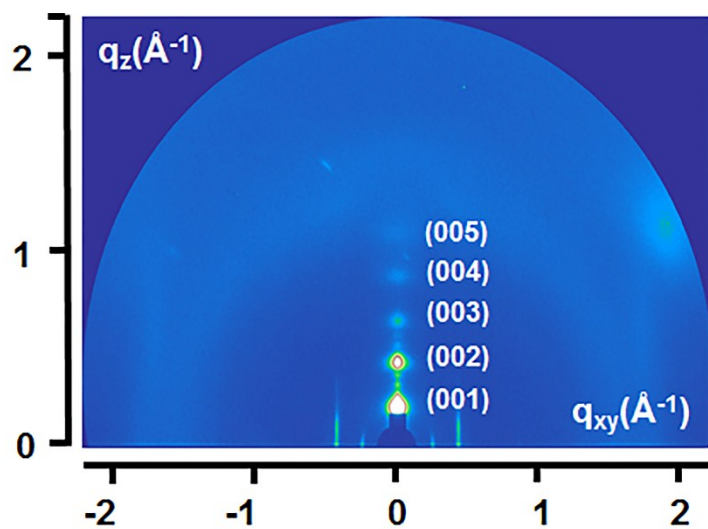


Figure S6. GIXD image of dichlorobenzene-based film of PNDI-TVT.

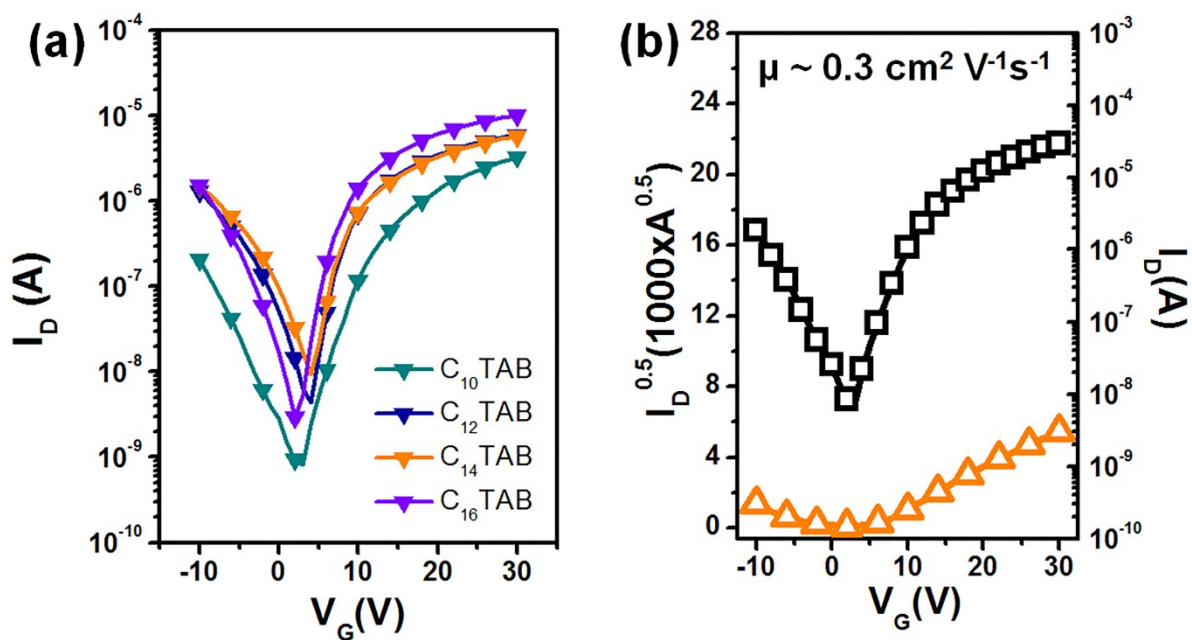
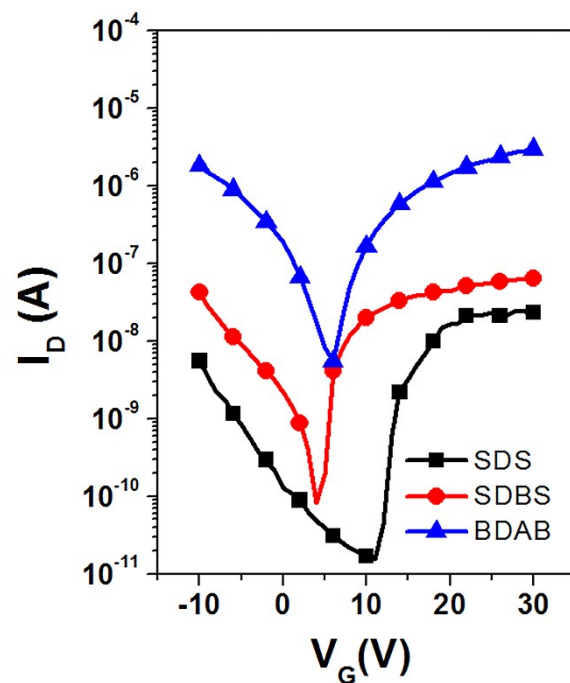
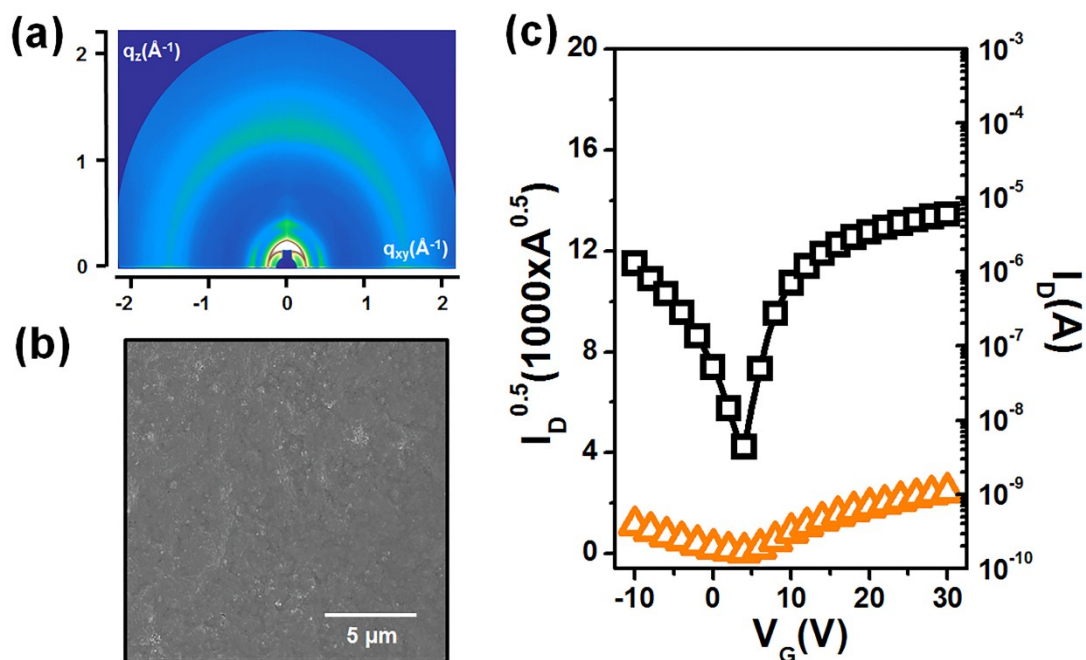


Figure S7. (a) The n-type transfer characteristics of colloid-based PFET using  $C_{10}$ TAB-,  $C_{12}$ TAB-,  $C_{14}$ TAB- and  $C_{16}$ TAB-based colloids of PNDI-TVT. (b) The n-type transfer characteristics of PFET fabricated from completely dissolved solution of PNDI-TVT in dichlorobenzene. The transfer curve is measured at saturated condition ( $V_{DS} = 30V$ ) and the extracted mobility from transfer curve in fig. (b) is  $0.3 \text{ cm}^2V^{-1}s^{-1}$ .



**Figure S8.** The n-type transfer characteristics of colloid-based PFET using SDS-, SDBS-, BDAB-based colloids of PNDI-TVT.



**Figure S9.** (a) GIXD pattern image and (b) SEM image of colloid-based film cast from TBAB-colloid solution of PNDI-TVT. (c) Transfer characteristics of colloid-based PFET of PNDI-TVT measured at n-type saturation condition ( $V_{DS} = 30V$ ).

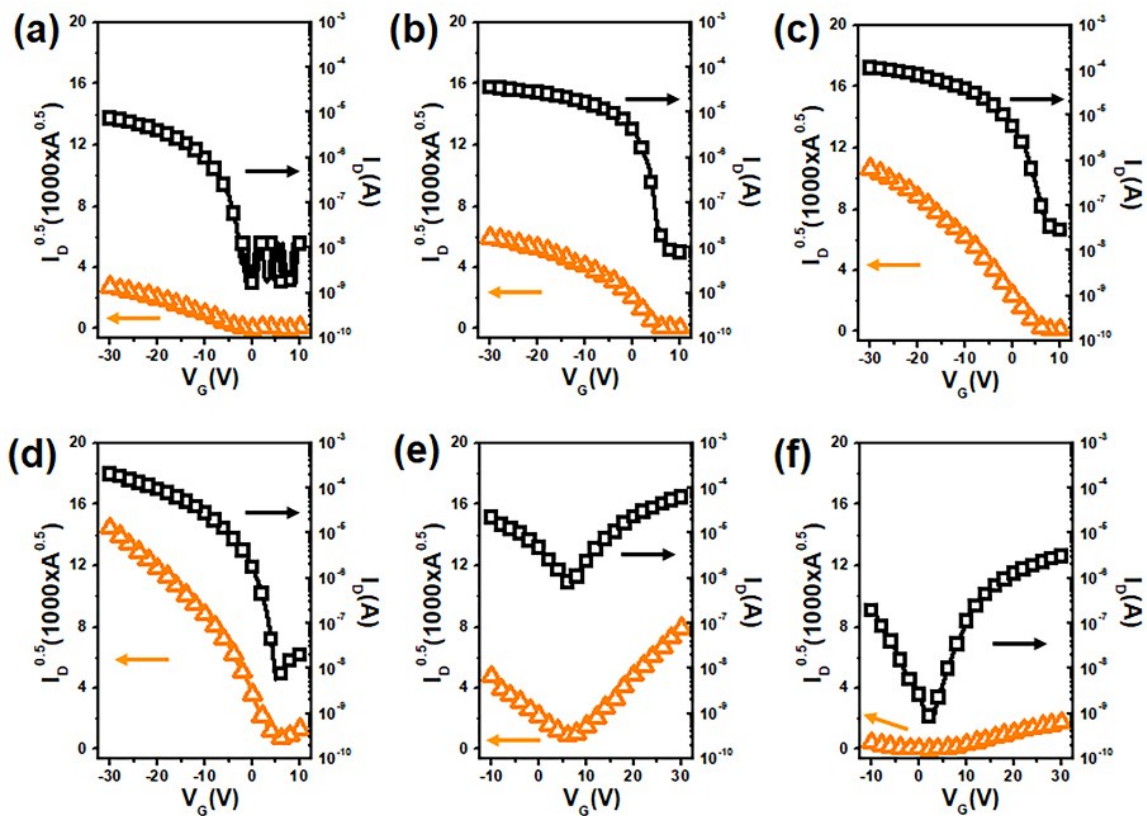


**Figure S10.** Transfer characteristics of PFET cast from completely dissolved solution by good solvent. The transfer curves measured at saturation condition using p-type polymers (a-d): (a) P3HT, (b) PBTTT, (c) PIID-SVS, (d) PDPP-SVS, ambipolar polymer: (e) PDPP-CN-TVT and n-type polymer: (f) PNDI2OD-T2. For p-type, ambipolar and n-type measurements,  $V_{DS} = -30V$ ,  $V_{DS} = -30V$  and  $V_{DS} = 30V$  were applied, respectively.

## 1. Materials

All the cationic, anionic, nonionic surfactants, P3HT and PBTTT were purchased from Sigma-Aldrich. PNDI2OD-T2 was purchased from 1-Material Inc. The PNDI-TVT, PIIID-SVS, PDPP-SVS and PDPP-CN-TVT were prepared following the previously reported synthetic protocol.

## 2. Colloid preparation

The PNDI-TVT of 5 mg was dissolved in chloroform of 2 ml. Surfactants were dissolved in DI-water of 6 ml and added to a solution of PNDI-TVT in vial (20 ml). The amount of surfactant used is listed in Table 1. The solution was stirred for 1 min and sonicated for 1 min with a Branson Model 8510 Ultrasonic Cleaner. This procedure was repeated until the color of the solution no longer changed, after which, the mixture was stirred for 1 hour. Finally, chloroform was fully evaporated at 65 °C.

## 3. PFET fabrication

The active layer was deposited from the colloidal solution by spray coating on an OTS-treated SiO<sub>2</sub>/Si substrate. The resultant film was dipped in ethanol for 3 min and annealed at 200°C for 10 min. Finally, the source/drain electrode was deposited by thermal evaporation. The channel W/L ratio was 10 with a channel width of 1500 μm, and a channel length of 150 μm.

## 4. Complementary inverter fabrication

The shadow mask for spray coating was prepared on the OTS-treated SiO<sub>2</sub>/Si substrate. The PBTTT thin film was deposited from the its colloidal solution by spray coating. By changing the shading of the mask, the PNDI-TVT thin film was deposited from the its colloidal solution by spray coating. The resulting film was dipped in ethanol for 3 min and annealed at 200°C for 10 min. Finally, the source/drain electrode was deposited by thermal evaporation. The W/L ratio of both channels is equal to 10 (channel width = 1000 μm, channel length = 100 μm).

## 5. Photodiode fabrication

A solution of 60 mg of C<sub>16</sub>TAB dissolved in 6 mL of DI-water was prepared. To this, 40 mg of P3HT in 2 mL chloroform was added. The solution was stirred for 1 min and sonicated. This procedure was repeated until the color of the solution no longer changed. After this, the mixture was stirred for 1 hour. Finally, chloroform was completely evaporated at 65°C. ITO-patterned glass substrates with a sheet resistance of ≈15 Ω sq<sup>-1</sup> were cleaned with aqueous hydrochloric acid, followed by sequential sonication in MucasoITM solution, deionized water, acetone, and isopropanol. Cleaned substrates were treated by O<sub>2</sub> plasma. A ZnO sol gel was prepared by dissolving 1096 mg of Zn(OAc)<sub>2</sub> (Sigma-Aldrich) in 10 mL of 2-methoxyethanol (Sigma-Aldrich) and addition of 0.28 mL of ethanolamine (Sigma-Aldrich). The solution was then stirred at room temperature for 1 h. The ZnO solution was spin-coated onto the substrates at 2000 rpm for 30 s to form a thin film and annealed for 30 min at ambient temperature. The prepared P3HT colloid solution was concentrated by centrifugation using UFC500324 Amicon Ultra Centrifugal Filters. The concentrated colloid solution was spin-coated onto the ZnO-coated substrate at 1000 rpm for 40 s. The resultant film was dipped in ethanol for 3 min. The devices were finished by evaporating 30 nm of MoO<sub>3</sub> and 200 nm of Au as the top electrode under a vacuum of ~2 × 10<sup>-6</sup> torr. The active area of the cells was 0.09 cm<sup>2</sup>.

## 6. Characterization

SEM images of top surface and cross-section were obtained using High Resolution (XHR) Field Emission Scanning Electron Microscope (SU8020/Hitachi) and focused ion beam technology. The hydrodynamic diameter in aqueous solution was measured by zetasizer, (Nano-ZS90/Malvern). Fourier Transform Infrared Spectroscopy (FT-IR) absorbance peaks were acquired using an FT-IR spectrometer (FT/IR 4700/JASCO). The GIXD measurements were performed using the PLS-II 3C, 9A U-SAXS beamline at the Pohang Accelerator Laboratory (PAL) in Korea. The X-rays coming from the in-vacuum undulator (IVU) were monochromated (E = 11.07 keV) using Si(111) double crystals and then focused at the detector position using a K-B focusing mirror system. The horizontal and vertical beam size was 300 (H) μm and 30 (V) μm, respectively. The incidence angle (α<sub>i</sub>) was adjusted to 0.12°, which is above the critical angle. GIXD patterns were recorded with a 2D CCD detector (Rayonix. SX-165). The diffraction angles were calibrated using pre-calibrated sucrose (Monoclinic,

P21) and the sample-to-detector distance was approximately 229 mm. The electrical characteristics of the PFETs and complementary inverter were measured using semiconductor parameter analyzer (Keithley 4200A-SCS/Keithley). Electrical characteristics of photodiode were measured using a Keithley 2400 Source Meter for two-terminal measurements both in dark and under illumination from a 150 W xenon arc lamp assembled with a 1/8 m monochromator, Stanford Research SR830 Lock-in Amplifier, AFG310 arbitrary function generator (Tektronix) and an OEM infrared green laser source (LSR532NL-300)

## 7. Specific measurement methods of photodiode

### 7.1 Noise current measurement

The noise current was measured with a Stanford Research SR830 Lock-In amplifier following the reported method.<sup>1</sup> The estimated shot noise limit( $i_{ns}$ ) and thermal noise limit( $i_{nt}$ ) obtained using

$$i_{ns} = \sqrt{2eBi_d} \quad (S1)$$

where B is the bandwidth,  $i_d$  is the dark current, and

$$i_{nt} = \sqrt{4k_B T B / R} \quad (S2)$$

where  $k_B$  is the Boltzmann constant,  $T$  is the temperature, and  $R$  is the series resistance. The measured noise current was found to be slightly higher than shot noise limit, implying that the noise is mostly governed by shot noise, as shown in Fig. 10g.

### 7.2 3dB bandwidth

The 3 dB bandwidth ( $\Delta f$ ) measured based on the dynamic responses of the photodiodes is directly related to the upper limit of the response speed by

$$\Delta f = 0.35/t_{\text{rising}} \quad (S3)$$

where  $t_{\text{rising}}$  is the rise time of the photocurrent after light exposure by a laser diode (520 nm) modulated by AFG310 arbitrary function generator (Tektronix).<sup>2</sup>

### 7.3 Linear dynamic range (LDR)

The LDR, which reflects the dynamic range of a photodiode under varying light intensity, can be calculated with the formula

$$\text{LDR} = 20 \log(j_{\text{max}}/j_{\text{min}}) \quad (S4)$$

where  $j_{\text{max}}$  and  $j_{\text{min}}$  are the maximum and minimum detectable current densities, respectively.<sup>3</sup> All measurements were performed by the 150 W xenon arc lamp and laser diode (520 nm)

## 8. Reference

1. J. P. Clifford, G. Konstantatos, K. W. Johnston, S. Hoogland, L. Levina, E. H. Sargent, *Nat. Nanotechnol.* 2009, **4**, 40-44.
2. A. Ben-David, *Appl. Opt.* 1996, **35**, 1531-1536.
3. R. D. Jansen-van Vuuren, A. Armin, A. K. Pandey, P. L. Burn, P. Meredith, *Adv. Mater.* 2016, **28**, 4766-4802.